

Singlet-Triplet Mixing in the $n = 3$ States of Helium[†]

Daniel Krause, Jr. and Edward A. Soltysik

Physics Department, University of Massachusetts, Amherst, Massachusetts 01002

(Received 20 October 1971; revised manuscript received 3 January 1972)

We have measured the energy-independent ratio of the proton apparent-excitation cross sections between corresponding triplet and singlet states of helium for the $n = 3$ level. In the Russell-Saunders description of the states of helium, proton excitation of triplet states is forbidden; i. e., $\Delta S = 1$ transitions are not allowed (Wigner spin rule). However, the spin-orbit interaction for the two electrons in helium mixes the spin states. Thus, there is a small singlet component in the triplet-state wave function. The square of the small singlet-triplet mixing parameter $\gamma(3^3X)$ is equal to the ratio of the proton excitation cross sections to corresponding triplet and singlet states, i. e., $\gamma^2(3^3X) = \sigma_p(3^3X)/\sigma_p(3^1X)$. The symbol X refers to the orbital angular momentum states S , P , or D . If we designate the ratio of the proton apparent-excitation cross sections $Q_p(3^3X)/Q_p(3^1X)$ by $\beta^2(3^3X)$, then $\beta^2(3^3X) = \gamma^2(3^3X) + (\text{cascade contributions})$. Our results for $\beta^2(3^3X)$ for the $n = 3$ states of helium are as follows: $\beta^2(3^3S) = 0 \pm 0.0002$, $\beta^2(3^3P) = 0.0028 \pm 0.0007$, and $\beta^2(3^3D) = 0.06 \pm 0.014$.

INTRODUCTION

In the Russell-Saunders (LS) coupling scheme, the stationary states of helium are described as either spin 0 (singlet) or spin 1 (triplet). It is as a consequence of the LS coupling scheme, therefore, that electromagnetic transitions between singlet and triplet terms are forbidden. However, even as early as 1922, Lyman¹ observed the helium line $\lambda = 591.5 \text{ \AA}$, which has been interpreted as the intercombinational line corresponding to the transition $2^3P_1 - 1^1S_0$. In addition, Jacquinet² observed the intercombinational line $\lambda = 5874.463 \text{ \AA}$ corresponding to the transition $3^1D_2 - 2^3P_1$. Also, Herzberg,³ besides observing these two intercombinational lines, reported an additional intercombinational line $\lambda = 6679.683 \text{ \AA}$ corresponding to the transition $3^3D_2 - 2^1P_1$. Thus, the LS coupling scheme is not strictly valid even for the low-lying states of helium. Instead we have states of helium which have a small singlet-triplet mixing. This small mixing is due to the spin-orbit interaction for the two electrons of helium.

Similarly, within the Russell-Saunders description, when protons interact with spin-0 ground-state helium atoms via the Coulomb force, only states with the same spin as the ground state can be excited. This $\Delta S = 0$ rule, the so-called Wigner spin rule,⁴ excludes the production of triplet ($S = 1$) states of helium under proton impact. However, because the spin-orbit interaction couples the spin-0 and spin-1 states, there is a small singlet-triplet mixing. Consequently, the Wigner spin rule will not strictly exclude direct proton excitation of triplet states of helium. Measurements of direct proton excitation cross sections to triplet states of helium yield information on the extent to which the spin-orbit interaction has mixed a singlet component into the triplet wave function. In this paper

we present our quantitative measurements of the cross sections for the direct excitation of the 3^3S , 3^3P , and 3^3D states of helium by proton impact.

At least to first order, we may write the more exact "triplet"-state wave function $\psi_t(\alpha)$ as a sum of a pure triplet ($S = 1$) wave function $\phi_t(\alpha)$ plus a small amount of a pure singlet ($S = 0$) wave function⁵ $\phi_s(\alpha)$:

$$\psi_t(\alpha) \cong \phi_t(\alpha) + \gamma\phi_s(\alpha) + \dots \quad (1)$$

The small mixing coefficient γ is due to the spin-orbit interaction for the two electrons, and $\alpha \equiv \{nlj\}$ refers to the additional quantum numbers specifying the state. Although the first-order correction to the wave function involves an infinite sum over spin-0 states, all with the same value of the total angular momentum j , the dominant term in the summation [shown in Eq. (1)] is the one whose energy eigenvalue is closest to the triplet state under consideration.⁵ Thus, for the "triplet" state $\psi_t(nlj)$ the dominant correction to $\phi_t(nlj)$ arises from the corresponding singlet state $\phi_s(nlj)$.

In this paper we are concerned with the ratio $\sigma_p(\alpha, S = 1)/\sigma_p(\alpha, S = 0)$ of the proton excitation cross sections between corresponding triplet and singlet states of helium. It follows from the above paragraph that $\sigma_p(\alpha, S = 1)/\sigma_p(\alpha, S = 0) = \gamma^2(\alpha)$. A consequence of the above reasoning is that the cross-section ratio $\sigma_p(\alpha, S = 1)/\sigma_p(\alpha, S = 0)$ is a number independent of the proton beam energy, which measures the square of the singlet-triplet mixing coefficient of the triplet state $\psi_t(\alpha)$.

Theoretical calculations of $\gamma(\alpha)$ have been reported for many states of helium.⁵⁻⁹ An experimental determination of the proton cross-section ratio $\sigma_p(\alpha, S = 1)/\sigma_p(\alpha, S = 0)$ then provides a direct comparison with these calculations. In the experiment reported in this paper, we are only able to obtain the ratio of the apparent proton cross

sections $Q_p(\alpha, S=1)/Q_p(\alpha, S=0)$. If we call this ratio $\beta^2(\alpha)$, then $\beta^2(\alpha) = \gamma^2(\alpha) + (\text{cascade contributions})$. The cascade contributions result from the direct proton excitation of higher "triplet" states followed by radiative cascade down to the α state. Again, this direct proton excitation of higher "triplet" states occurs because there is a breakdown of the LS coupling scheme in the higher states. Thus $\beta^2(\alpha)$ is an upper limit to the extent of the breakdown of the LS coupling scheme in the state α .

A search of the literature reveals that, while many investigators report not observing triplet-state excitation of helium under proton and/or deuteron bombardment, there are a few investigators who do report observing such triplet-state excitation. Through careful analysis of the hydrogen-atom component of their beam (which can directly excite triplet states by electron exchange), Van Eck, de Heer, and Kistemaker¹⁰ were able to report the value $Q_p(3^3P)/Q_p(3^1P) = 0.0041$ at a proton beam energy of 30 keV. Sternberg and Tomas¹¹ measured the deuteron apparent-excitation cross sections $Q_D(3^3D)$, $Q_D(4^1D)$, and $Q_D(5^1D)$. If we accept the validity of the n^{-3} cross-section scaling law, we obtain from their measured values a crude estimate for the ratio $Q_D(3^3D)/Q_D(3^1D) \approx 0.04$. At a proton beam energy of 200 keV, Hughes, Waring, and Fan¹² reported the apparent-excitation cross sections $Q_p(3^1P)$, $Q_p(3^3P)$, $Q_p(3^3D)$, $Q_p(4^1D)$, and $Q_p(5^1D)$. Again, if we use the n^{-3} scaling law, we obtain from their measured values the estimates $Q_p(3^3P)/Q_p(3^1P) \approx 0.006$ and $Q_p(3^3D)/Q_p(3^1D) \approx 0.38$. In an earlier paper,¹³ we reported that the triplet-singlet cross-section ratio was moderately constant in the beam energy range from 2 to 25 keV for the $n=3$ S and D states. However, our cross sections were measured in arbitrary units, so that no number was presented for the cross-section ratio.

Since it is expected that the cross section for the proton excitation of triplet states is small [i. e., $[\sigma_p(\alpha, S=1)/\sigma_p(\alpha, S=0)] = \gamma^2 \ll 1$], care must be taken to account properly for triplet-state populations which may arise from processes other than direct proton excitation. Generally speaking, these other effects arise from secondary collisions and can be minimized by performing the experiment at low helium target-gas pressures. Specifically, the hydrogen-atom component in the beam, resulting from the charge-exchange process $p + \text{He} \rightarrow \text{H} + \text{He}^+$, may in fact excite triplet states of helium by electron exchange, with no violation of the Wigner $\Delta S=0$ spin rule. Also, "collisions of the second kind" may lead to triplet-state excitation when directly excited singlet-state helium transfers its excitation to a triplet state through collisions with ground-state atoms. The apparatus designed for

the experiment reported here enables us to account for all secondary channels to the triplet states except radiative cascade. We are able to isolate the direct proton contribution to the triplet-state populations for the 3^3S , 3^3P , and 3^3D states of helium, which provides us with a measurement of β^2 for these states.

APPARATUS

A schematic diagram of the proton accelerator used in the experiment reported here is shown in Fig. 1. The accelerator is presently operated in the beam energy range $10 < E < 80$ keV with a proton beam current $5 < I_p < 40$ μA . The proton beam is deflected through a 45° angle by the analyzing magnet and immediately enters the gas target chamber through two 0.5-cm-diam collimating apertures. Figure 2 shows the details of the target chamber. By placing the entrance aperture as close as possible to the analyzing magnet, and by pumping with a fast diffusion pump in the immediate vicinity of the entrance aperture, we minimize the formation of hydrogen atoms in the beam, owing to charge-exchange scattering, prior to entrance into the target chamber. This ensures a pure proton beam upon entrance into the target chamber. This point is discussed further in the section entitled Beam Composition.

During an experimental run, helium gas is continuously leaked into the chamber, which is pumped on by a N. R. C. 4-in. oil diffusion pump backed by a large Welch mechanical pump. The chamber gas pressure is continuously monitored by a N. R. C. ionization gauge.

The target chamber is 42 cm long. Its sides consist of two 35-cm-long windows through which light, produced by the collisions of the beam particles with the target gas, can be viewed. The beam is collected in an electrically biased Faraday cup assembly, which is movable between 6 cm from the analyzing magnet and 30 cm from the analyzing magnet. The Faraday cup assembly also contains two 0.5-cm-diam collimating apertures which define a small volume of beam to be viewed by the

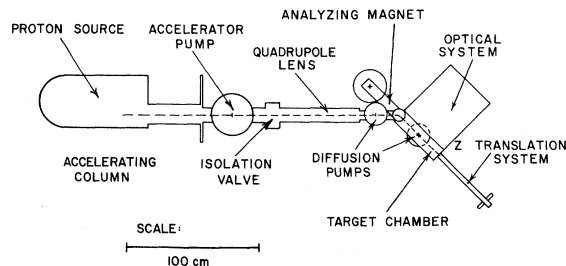


FIG. 1. Schematic diagram of the accelerator and experimental arrangement.

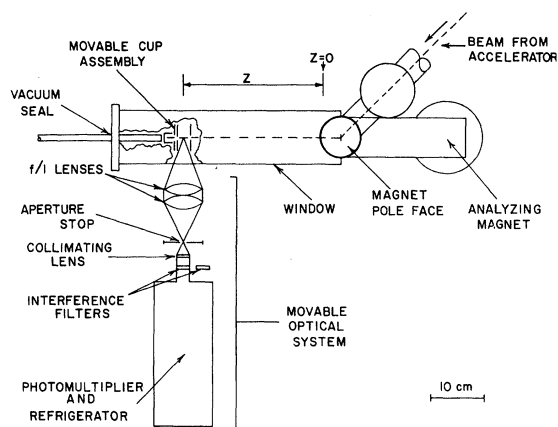


FIG. 2. Detail of the collision chamber and optical system.

optical detection system.

The entire optical system is mounted on a track inside a light tight box located outside the vacuum windows. This optical system moves in synchronization with the Faraday cup assembly. The optical system consists of two 7.3-cm-diam $f/1$ lenses which focus light from an adjustable aperture stop which accepts light from a beam length of 0.5 cm. Light passing through the aperture stop is formed parallel to the axis of the optical system by a third 2.5-cm-diam $f/1$ lens. The light then passes through an appropriate interference filter and onto the photocathode of the photomultiplier (PM). The PM tube is a thermoelectrically cooled E. M. I. 9558QB tube which has an S-20 response. The electrical pulses for the PM tube are appropriately amplified and counted on a scaler.

BEAM COMPOSITION

The fast hydrogen atoms, produced in the beam by charge-exchange scattering of protons on the target helium gas, excite triplet states through electron exchange without violating the Wigner spin-conservation rule. Thus, a significant proportion of the observed light arising from triplet states may be due to hydrogen-atom excitation. In order to identify that part of the observed light intensity which is due to direct proton excitation, it is necessary to know the hydrogen-atom component of the beam.

The beam-analyzing magnet deflects only protons into the proper trajectory down the center of the collision chamber (see Fig. 2.). However, as the protons move through the target gas, there is a buildup of hydrogen atoms in the beam due to charge-exchange scattering. Thus, at some point Z in the target chamber, the beam consists predominantly of protons plus a small fraction of hy-

drogen atoms. At the low target-gas pressures employed in this work ($5 \times 10^{-5} < p < 10^{-4}$ Torr), the helium-atom number density N is sufficiently small so that the hydrogen-atom component of the beam at the point Z is adequately described by the linear relationship¹⁴

$$j_H(NZ) \cong j_p(0)\sigma_{10}(E)NZ, \quad (2)$$

where $j_H(NZ)$ is the hydrogen-atom current density, $j_p(0)$ is the proton current density at the point $Z=0$, Z is the distance downstream into the target chamber measured from the point $Z=0$ where the beam is pure protons, and $\sigma_{10}(E)$ is the energy-dependent charge-exchange cross section. [See Ref. 14 for measurements of $\sigma_{10}(E)$.]

In order to locate the point in our chamber where the beam is pure protons (i. e., $Z=0$), we have done the following: (i) By studying the possible trajectories of the proton beam in the magnetic field of the analyzing magnet (see Fig. 2), we determined that any hydrogen atoms produced in the beam further upstream than 0.75 cm before the entrance aperture would be excluded from entering the target chamber by the entrance aperture. (ii) We have measured the buildup of the hydrogen line H_β ($\lambda = 4861 \text{ \AA}$) as a function of the gas number density N and the distance Z for a number of different beam energies. The production of hydrogen atoms in the $n=4$ state arises from the charge-exchange process $p + \text{He} \rightarrow \text{H}(n=4) + \text{He}^+$. Since the S , P , and D angular momentum states associated with the $n=4$ energy level are mixed by the fringing field of the analyzing magnet, the decay from the resulting mixed state is characterized by a single radiative lifetime τ .¹⁵ The observed light intensity $I(H_\beta)$, per unit number density N and per unit beam current density j_p , is accurately described by the relationship $I(H_\beta) = \alpha(E) [1 - e^{-Z/v\tau}]$, where v is the beam velocity, and $\alpha(E)$ is proportional to the charge-exchange cross section into the $n=4$ level. In order to minimize errors associated with measurements of N and j_p at the point of observation, we measured the light intensity arising from the $3^1S - 2^1P$ ($\lambda = 7281 \text{ \AA}$) transition in helium along with the measurement of the H_β line. (We have already determined that the light from the helium transition $3^1S - 2^1P$ was independent of Z and proportional to the product Nj_p .) By taking the ratio of the light intensity $I(H_\beta)$ to the light intensity $I(3^1S)$, we obtain an accurate measurement for $I(H_\beta)/I(3^1S)$ free from errors due to uncertainties in the measurement of the pressure and beam current at the point of observation. The ratio $I(H_\beta)/I(3^1S)$ is proportional to the ratio of the two corresponding apparent cross sections $Q(H_\beta)/Q(3^1S)$. Shown in Fig. 3 are typical data for $Q(H_\beta)/Q(3^1S)$ at two different beam energies as a function of Z . For all beam energies ($10 < E < 80 \text{ keV}$) the measured ratio $Q(H_\beta)/Q(3^1S)$ as a

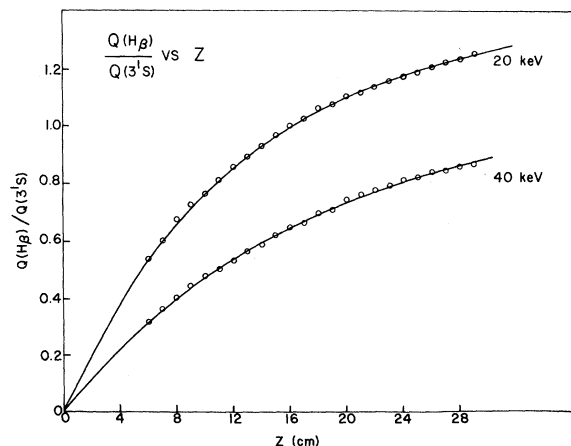


FIG. 3. Position of $Z=0$ in our apparatus, where the beam consists of pure protons, is established by the fit of our measured values for the ratio $Q(H\beta)/Q(3^1S)$, shown by the open circles, to the equation $y = A[1 - e^{-Z/\nu\tau}]$, which is the solid curve shown.

function of Z is accurately described by the relation $Q(H\beta)/Q(3^1S) \propto [1 - e^{-Z/\nu\tau}]$, with the point $Z=0$ located (0.50 ± 0.25) cm upstream from the target chamber entrance aperture.

Thus, with the point in our chamber where the beam is composed purely of protons identified (i. e., $Z=0$ is located (0.50 ± 0.25) cm upstream from the entrance aperture to the target chamber), the distance Z appearing in all figures and subsequent discussion is measured from this point in our chamber.

We have verified the linear buildup of the hydrogen-atom component of the beam by measuring the ratio of the apparent cross section of the 3^3S state of helium to the apparent cross section of the 3^1S state of the helium by the beam particles. Since for the 3^3S state of helium there is no spin-orbit interaction, there will be no breakdown of the LS coupling scheme. Thus, we expect that there will be no excitation of the 3^3S state of helium by the proton component of the beam. The only excitation will then be due to the small hydrogen-atom component of the beam, which may proceed via electron exchange without violating the spin-conservation rule. Thus, the observed light intensity will be proportional to the hydrogen-atom current density. The 3^1S state is easily excited by protons, so at these low number densities, where the beam consists predominantly of protons, the observed light intensity of the 3^1S state will be proportional to the proton current density j_p . Consequently, the ratio of the light intensity from the 3^3S state of helium to the light intensity from the 3^1S state of helium (both excited by the same beam) is simply proportional to NZ . Shown in Fig. 4 is our measured

ratio of the apparent cross sections $Q(3^3S)/Q(3^1S)$ at three different gas pressures as a function of the distance downstream Z . Examination of Fig. 4 reveals that our understanding of the beam composition is correct. Note that the point of intersection of these lines is the point $Z=0$, and that the 3^3S light intensity at this point is zero. This supports our other observation that the buildup of hydrogen atoms does in fact begin at $Z=0$ located (0.50 ± 0.25) cm upstream from the entrance to the chamber.

EXPERIMENTAL PROCEDURE

At a fixed beam energy E , and helium target-gas pressure p , the light intensity resulting from the interaction of the beam and the target-gas atoms was measured as a function of the distance Z . Measurements were made in the energy range $10 < E < 80$ keV in 10 keV steps, and at a number of different target-gas pressures in the range $5 \times 10^{-5} < p < 5 \times 10^{-4}$ Torr. Simultaneously, the proton beam current was measured with the Faraday cup assembly which moves in synchronization with the movable light detection system (see Fig. 2). Helium gas was continuously leaked into the collision chamber through a fine control leak valve, and the pressure was monitored with a N. R. C. ionization gauge. At each position of the detector assembly, alternately the intensity of the light arising from the triplet transition under study and the light arising from the $3^1S \rightarrow 2^1P$ transition were measured. The alternate measurement of the two wavelengths was accomplished by a mechanism which interchanged the interference filters used to select the wavelength to be measured. Two minute counts were taken for each wavelength and each Z position from

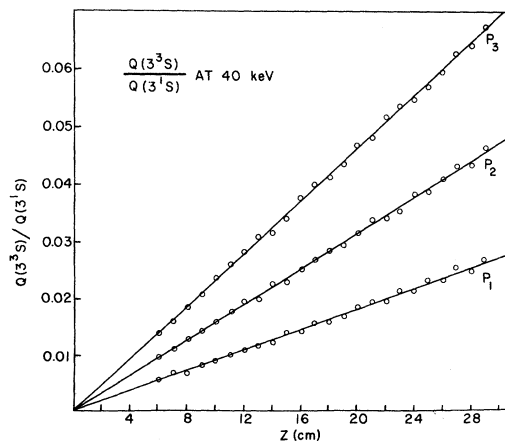


FIG. 4. Open circles show the measured values for the ratio $Q(3^3S)/Q(3^1S)$ as a function of the distance Z , at a beam energy of 40 keV for three different target-gas pressures. The solid lines are least-squares fits to the observed data.

$Z = 6$ cm to $Z = 30$ cm at intervals of 2 cm. The light arising from the $3^1S \rightarrow 2^1P$ transition is called the reference line because the intensity of this light has been observed to be directly proportional to the product of the proton current and the helium-gas number density at the point of observation. Thus, by taking the ratio of the light intensity arising from the triplet transition under study $I(3^3X)$ [$X = S, P,$ or D] to the light intensity arising from the reference line $I(3^1S)$, we obtain an accurate measurement proportional to the ratio of the corresponding apparent cross sections [i. e., $I(3^3X)/I(3^1S) \propto Q(3^3X)/Q(3^1S)$] free from errors due to any uncertainties in the measurement of the pressure and the beam current.

Before the interference filters were employed, we made measurements to ensure that the interference filters had sufficiently narrow bandpass so that they did in fact transmit only the desired wavelength. The spectrum of light produced by the beam passing through helium gas was analyzed with an Engis large-aperture grating monochromator (model S 05-01), with a grating blazed for 7000 \AA . All of the observed lines were identified as either helium lines or hydrogen Balmer lines. This spectrum determined what bandwidth filters were necessary to ensure adequately that only light of the appropriate wavelength would be transmitted to the PM tube. Thus, we found that some transitions required 10-\AA bandwidth filters full width at half-maximum, while 50-\AA filters were adequate for others.

The efficiency of the optical detection system is dependent on the transmission of the filters and the optical system, as well as on the quantum efficiency of the PM tube. The efficiency at each of the wavelengths observed in this experiment, relative to the efficiency of the reference line, was established by measuring the light intensity resulting from the interaction of an H_2^+ beam with the helium gas. Using reported¹⁶ values of the H_2^+ cross sections, we then established the relative efficiencies at the two different wavelengths.

ANALYSIS

At the low helium target-gas densities employed in this experiment, the population of the 3^3X state ($X = S, P,$ or D) is determined by four identifiable processes: (i) radiative loss and radiative cascade, (ii) direct proton excitation, (iii) direct hydrogen-atom excitation, and (iv) excitation transfer. The small direct proton excitation contribution which we are concerned with here is directly proportional to the gas number density N . Since the hydrogen-atom component of the beam is directly proportional to the product NZ [see Eq. (2)], the direct hydrogen-atom excitation contribution is proportional to $N(NZ)$. The excitation transfer contribution,

which involves only a second collision, is of course proportional to N^2 . It then follows from the continuity equation at equilibrium conditions that the apparent cross section $Q(3^3X)$ must be of the following form:

$$Q(3^3X) = Q_p(3^3X) + B[Z + Z_0]N, \quad (3)$$

where the apparent cross section $Q(3^3X)$ is defined by

$$Q(3^3X) \equiv N(3^3X)/Nj\tau(3^3X), \quad (4)$$

in which $N(3^3X)$ is the population density of the 3^3X state, j is the proton beam current density, and $\tau(3^3X)$ is the lifetime of the 3^3X state. We have defined $Q_p(3^3X) \equiv \sigma_p(3^3X) + (\text{radiative cascade from above})$, where $\sigma_p(3^3X)$ is the direct proton excitation cross section to the 3^3X state. The number B measures the extent of the hydrogen-atom contribution to the 3^3X state, and BZ_0 measures the extent of the excitation transfer contribution to this state. As we will now see, it is not necessary at this point to consider the exact form of the expressions for B and BZ_0 in order to obtain the proton contribution $Q_p(3^3X)$. However, for those who are interested, we refer to a previous paper¹⁷ for a discussion giving explicit expressions for B and Z_0 . It should be noted in passing (see Figs. 4-6) that $Z_0 \approx 0$ for the 3^3S and 3^3P states, whereas for the 3^3D state it is not zero but a well defined function of the beam energy.

All of our data are in fact described by the relationship given in Eq. (3). Figures 4-6 show some typical data taken at one of the energies which we used in our measurement. For each of the states 3^3X , measurements were made similar to those shown in Figs. 4-6 at 10 keV intervals of the beam

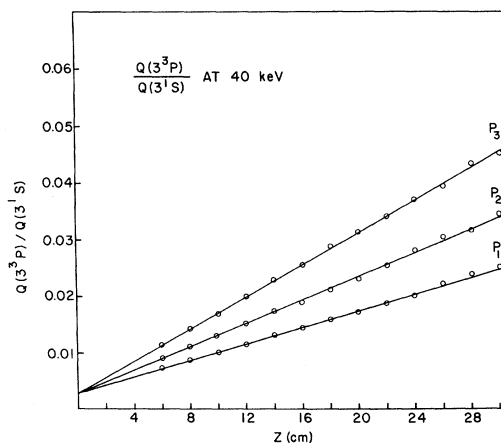


FIG. 5. Open circles show the measured values for the ratio $Q(3^3P)/Q(3^1S)$ as a function of the distance Z , at a beam energy of 40 keV, for three different target-gas pressures. The solid lines are least-squares fits to the observed data.

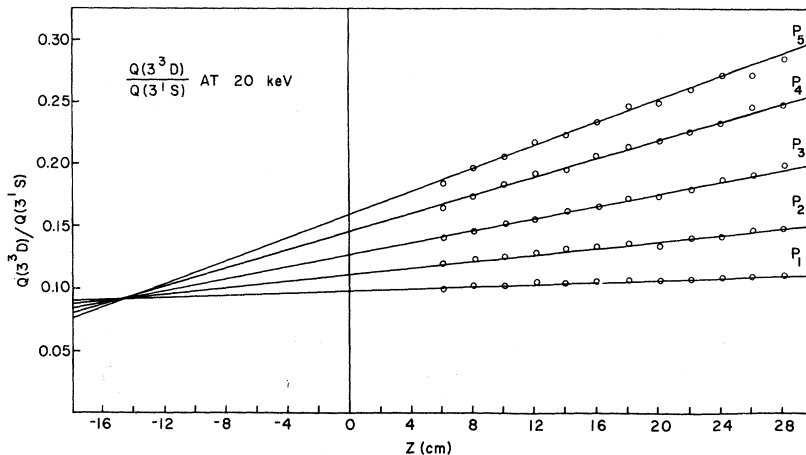


FIG. 6. Open circles show the measured values for the ratio $Q(3^3D)/Q(3^1S)$ as a function of the distance Z , at a beam energy of 20 keV, for five different target-gas pressures. The solid lines are least-squares fits to the observed data.

energy in the range from 10 to 80 keV. At different gas pressures, the straight lines describing the data points all intersect at the common point $Z = -Z_0$. Hence, experimentally, we identify $Q_p(3^3X)$ as the value of $Q(3^3X)$ at the point of intersection $Z = -Z_0$:

$$\begin{aligned} Q_p(3^3X) &= \sigma_p(3^3X) + (\text{radiative cascade}) \\ &= Q(3^3X)|_{Z=-Z_0}. \end{aligned} \quad (5)$$

Note that, for the purposes of minimizing the experimental error, we actually measure the ratio of the 3^3X apparent cross section to the 3^1S apparent cross section [i. e., $Q(3^3X)/Q(3^1S)$]. The reasons for doing this have already been discussed in the section entitled Experimental Procedure.

RESULTS

The experimental data are the measured intensity $I(\alpha)$ of the light of a given wavelength resulting from the interaction of the beam with the target helium gas. At a fixed beam energy E and gas pressure p , the intensity $I(3^3X)$ of the light arising from radiative transitions out of the 3^3X state is measured as a function of Z , along with a measurement of the intensity of the reference line $3^1S \rightarrow 2^1P$ ($\lambda = 7281 \text{ \AA}$). The ratio of the intensities of the two lines is proportional to the two corresponding apparent cross sections; that is, $Q(3^3X)/Q(3^1S) = \epsilon I(3^3X)/I(3^1S)$. The value of ϵ for each state $X = S, P,$ and D has been determined by measuring the light intensities $I(3^3X)$ and $I(3^1S)$ resulting from the interaction of the helium target gas and a H_2^+ beam, selected out of our accelerated beam by the analyzing magnet. For $Q(3^3X)$ and $Q(3^1S)$ we have used the measured values for the H_2^+ apparent cross sections reported by the Amsterdam laboratory.¹⁶ The ratio $Q(3^3X)/Q(3^1S)$ so determined is least-squares fitted to a linear function of Z for a number of different target-gas pressures p and

beam energies E . For each beam energy, the lines corresponding to different gas pressures have a common point of intersection. It is the value for $[Q(3^3X)/Q(3^1S)]_{Z=-Z_0}$ at the common point of intersection which gives us the contribution to the apparent cross section ratio due only to proton excitation [see Eqs. (3) and (5)]. The value of $\beta^2(3^3X)$ is then obtained by multiplying the measured ratio $[Q(3^3X)/Q(3^1S)]_{Z=-Z_0}$ by the appropriate energy-dependent singlet-singlet apparent cross-section ratio $Q_p(3^1S)/Q_p(3^1X)$ reported by Van den Bos of the Amsterdam laboratory.¹⁸ We then have

$$\begin{aligned} \beta^2(3^3X) &= \frac{Q_p(3^3X)}{Q_p(3^1X)} \\ &= \left[\frac{Q(3^3X)}{Q(3^1S)} \right]_{Z=-Z_0} \left[\frac{Q_p(3^1S)}{Q_p(3^1X)} \right]_{\text{Van den Bos}}. \end{aligned} \quad (6)$$

Our results for β^2 for the $3^3S, 3^3P,$ and 3^3D states are shown in Table I. Within the quoted experimental error, our values of β^2 for each state are energy independent in the range $10 < E < 80$ keV. For example, Fig. 7 shows some of our measured values of $\beta^2(3^3P)$ as a function of beam energy.

DISCUSSION OF RESULTS

The reported values for the error in our measurement of β^2 (see Table I) represent the average value of one standard deviation of all the measured values of β^2 . The statistical errors are greatest at beam energies where the charge-exchange cross section $\sigma_{10}(E)$ is greatest. This is due to the fact that slopes of the straight lines shown in Figs. 4–6 are greatest when the charge-exchange process ($p + \text{He} \rightarrow \text{H} + \text{He}^+$) has produced a large fraction of hydrogen atoms in the beam. Consequently, there is a larger uncertainty in the extrapolated point of intersection, so $Q_p(3^3X)/Q_p(3^1X) \equiv Q(3^3X)/Q(3^1S)|_{Z=-Z_0}$ will also have its error largest where $\sigma_{10}(E)$ is greatest. By taking the average of one

standard deviation for the measurement of β^2 at each beam energy, we obtain a reasonable estimate of the statistical error associated with our measurements of $\beta^2(3^3X)$. It is apparent from Eq. (6) that the error in $\beta^2(3^3S)$ results only from the statistical error in our measurement. However, for $\beta^2(3^3P)$ and $\beta^2(3^3D)$ we estimate that 75% of the quoted error (see Table I) is due to the uncertainty in the measurements reported by the Amsterdam laboratory.

As noted in the Introduction, since the singlet-triplet mixing ratio γ is dependent on the spin-orbit interaction, we expect $\gamma = 0$ for the 3^3S state; and our reported value for $\beta^2(3^3S) = \gamma^2(3^3S) + (\text{cascade contributions}) = 0 \pm 0.0002$ is consistent with this view. Also, the observation that $Z_0 = 0 \pm 0.25$ for all beam energies reaffirms that the excitation transfer mechanism is not an important factor in determining the population of the 3^3S state, since Z_0 is the parameter that measures the effect of excitation transfer [see Eq. (3)].

Our measurement of the proton triplet-singlet apparent cross-section ratio $Q_p(3^3P)/Q_p(3^1P) = \beta^2(3^3P) = 0.0028 \pm 0.0007$ indicates that there is a significant amount of singlet-triplet mixing into the 3^3P state. Also, since $Z_0 = 0 \pm 1.5$ for all beam energies, we conclude that excitation transfer is not a major mechanism in determining the population of the 3^3P state. However, since the square of the singlet-triplet mixing coefficient γ^2 is less than β^2 , i. e., $\beta^2(3^3P) = \gamma^2(3^3P) + (\text{cascade contributions})$, our measurement of $\beta^2(3^3P)$ provides only an upper limit for the mixing coefficient. Since $\beta^2 \approx 0$ for the n^3S states, these states cannot be directly excited by proton impact. Thus, the 3^3P state cannot be populated by cascade from upper

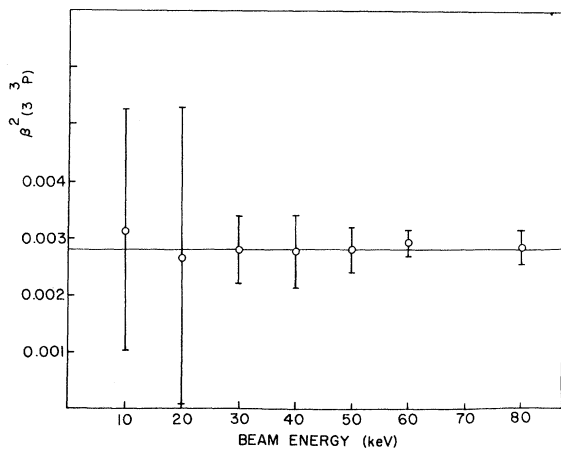


FIG. 7. Plot of some measured values of the square of the singlet-triplet mixing coefficient $\beta^2(3^3P)$ for the 3^3P state of the helium as a function of the beam energy.

TABLE I. Final results for the measured values of β^2 for the $n=3$ states of helium. Also shown is the measured value of the parameter Z_0 which measures the excitation transfer contribution to the particular state.

State	$\beta^2(3^3X)$	Z_0
3^3S	0 ± 0.0002	0 ± 0.25
3^3P	0.0028 ± 0.0007	0 ± 1.5
3^3D	0.06 ± 0.014	$Z_0 = Z_0(E)^a$

^aSee Ref. 17 for a complete discussion of the energy dependence of Z_0 for the 3^3D state.

n^3S states. However, the higher D states can be excited directly by protons and through radiative cascade contribute to the proton apparent cross section of the 3^3P state. Recent calculations^{6,7} show that γ^2 has essentially no n dependence but is strongly l dependent. We might, therefore, expect that β^2 will also not exhibit a strong n dependence. Thus, if we assume that $\beta^2(n^3D) \cong \beta^2(3^3D) = 0.06 \pm 0.014$, and if we use the measured^{10,18} n^1D proton cross sections for $n=4, 5$, and 6 and apply the n^{-3} scaling law to estimate the n^1D cross sections for larger n , then we estimate that the maximum cascade contribution to $\beta^2(3^3P)$ is ≈ 0.0015 . Recently, van den Eynde, Neimeyer, and Wiebes⁶ reported a value for $\gamma^2(3^3P) = 6.8 \times 10^{-8}$ —a value many orders of magnitude smaller than what we estimate from our measurements of β^2 .

The population of the 3^3D state is significantly influenced by the excitation transfer process [i. e., $Z_0 = Z_0(E) \neq 0$]. This fact has been thoroughly demonstrated by a number of investigators.^{17,19-21} Also, as has been pointed out by St. John and Fowler¹⁹ and van den Eynde, Niemeyer, and Wiebes,⁶ the higher F states of helium may be highly mixed, i. e., a rather complete breakdown of the Russell-Saunders coupling scheme for the F states. Thus, excitation of the so-called " n^3F " states by protons may be nearly as probable as the excitation of the n^1F states. If this is true, then it may be that a significant fraction of the 3^3D state apparent cross section which we observe is due to direct proton excitation of these higher " n^3F " states, followed by radiative cascade. We therefore can only conclude that our reported value of $\beta^2(3^3D) = Q_p(3^3D)/Q_p(3^1D) = 0.06 \pm 0.014$ represents an upper limit for $\gamma^2(3^3D)$. The reported calculations of van den Eynde, Niemeyer, and Wiebes,⁶ predict $\gamma^2(3^3D) = 8.8 \times 10^{-5}$.

In conclusion, our measurements of β^2 for the 3^3S , 3^3P , and 3^3D states of helium show, at least qualitatively, the dependence upon the angular momentum quantum number l which one expects. Since β is a parameter measuring the extent of singlet-triplet mixing due to the spin-orbit interaction, we expect and, in fact, do observe $\beta^2(3^3S)$

= 0 and also find $\beta^2(3^3S) < \beta^2(3^3P) < \beta^2(3^3D)$ (see Table I). However, we do report measuring sig-

nificantly larger values for $\beta^2(3^3P)$ and $\beta^2(3^3D)$ than would be expected from recent calculations.⁶

†This research was supported in part by the U. S. Air Force Office of Scientific Research under Grant No. AFOSR-69-1748.

¹T. Lyman, *Nature* **110**, 278 (1922).

²P. Jacquinot, *Compt. Rend.* **208**, 1896 (1939).

³G. Herzberg, *Proc. Roy. Soc. (London)* **248**, 309 (1958).

⁴E. Wigner, *Gott. Nachr. Math.-Phys. Kl.* **375** (1927).

⁵R. C. Elton, *Astrophys. J.* **148**, 573 (1967).

⁶R. K. L. van den Eynde, Th. Niemeier, and G. Wiebes, *Physica* (to be published).

⁷R. M. Parish and R. W. Mires, *Phys. Rev. A* **4**, 2145 (1971).

⁸G. W. F. Drake, *Phys. Rev.* **181**, 23 (1969).

⁹G. W. F. Drake and A. Dalgarno, *Astrophys. J.* **157**, 459 (1969).

¹⁰J. Van Eck, F. J. de Heer, and J. Kistemaker, *Physica* **30**, 1171 (1964).

¹¹Z. Sternberg and P. Tomas, *Phys. Rev.* **124**, 810 (1961).

¹²R. H. Hughes, R. C. Waring, and C. Y. Fan, *Phys. Rev.* **122**, 525 (1961).

¹³D. Krause, Jr. and E. A. Soltysik, *Phys. Rev.* **175**, 142 (1968).

¹⁴S. K. Allison, *Rev. Mod. Phys.* **30**, 1137 (1958).

¹⁵V. A. Ankudinov, S. V. Bobashev, and E. P. Andreev, *Zh. Eksperim. i Teor. Fiz.* **48**, 40 (1965) [*Sov. Phys. JETP* **21**, 26 (1965)].

¹⁶J. Van den Bos, G. Winter, and F. J. de Heer, *Physica* **44**, 143 (1969).

¹⁷D. Krause, Jr. and E. A. Soltysik, *Phys. Rev. A* (to be published).

¹⁸J. Van den Bos, G. Winter, and F. J. de Heer, *Physica* **40**, 357 (1968).

¹⁹R. M. St. John and R. G. Fowler, *Phys. Rev.* **122**, 1813 (1961).

²⁰J. D. Jobe and R. M. St. John, *J. Opt. Soc. Am.* **57**, 1449 (1967).

²¹R. J. Anderson, R. H. Hughes, and T. G. Norton, *Phys. Rev.* **181**, 198 (1969).

Set of Empirical Total Atomic Binding Energies B_Z , and Their Derivatives $\partial B_Z/\partial Z$, for All $Z \leq 18^*$

William Rubinson

Chemistry Department, Brookhaven National Laboratory, Upton, New York 11973

(Received 7 October 1971; revised manuscript received 6 March 1972)

A method is described whereby it is possible to make accurate empirical estimates of ionization potentials that are missing in Moore's "atomic energy levels," and so obtain empirical total atomic binding energies B_Z with estimated uncertainties less than 0.005%, for all $Z \leq 18$. These B_Z values are used to compute values of $\partial B_Z/\partial Z$, with quite small assigned uncertainties ($\sim 0.15\%$ for $Z \geq 12$). The relativistic Dirac-Hartree-Fock calculations of Mann reproduce these empirical values to within amounts a few times the uncertainties.

I. INTRODUCTION

There exists very little experimental material against which to compare the very extensive theoretical results now available on total atomic binding energies B_Z and their derivatives $\partial B_Z/\partial Z$. Theoretical values are available for all atomic numbers $Z \leq 103$,^{1,2} and even for the yet unknown atoms of atomic numbers $118 \leq Z \leq 135$ ³; the ionization energy data in Moore's well-known compilation of atomic energy levels⁴ suffice to compute experimental values of B_Z only for $Z \leq 8$. Consequently there is only a very meager basis for assessing the accuracy of the theoretical values, and one is at a loss to estimate the errors introduced by their use in other calculations, for

example, in calculations of mean atomic excitation energies in radioactive decay.^{5,6}

In the present work we provide some improvement on this state of affairs by producing a set of effectively experimental B_Z values for all $Z \leq 18$. As described in Sec. II, this is accomplished by a simple, accurate method of interpolation in, and extrapolation from, the ionization energy data in Moore's tables to obtain empirical estimates of missing ionization energies, with small errors assigned in an objective way. These estimated values are used to compute the empirically estimated B_Z values entered in Table III, where they are also compared with various theoretical values, in particular with the yet unpublished results of calculations by Mann² (quoted with his kind per-